

# Insight to UV-induced formation of laser damage on $\text{LiB}_3\text{O}_5$ optical surfaces during long-term sum-frequency generation

S. Möller, Ä. Andresen, C. Merschjann, B. Zimmermann, M. Prinz and M. Imlau

*University of Osnabrück, Department of Physics,  
Barbarastrasse 7, D-49069 Osnabrück, Germany*

[Stefan.Moeller@uos.de](mailto:Stefan.Moeller@uos.de)

**Abstract:** Microscopic investigations of UV-induced formation of laser damage on  $\text{LiB}_3\text{O}_5$  optical surfaces during long-term sum-frequency generation (SFG) uncovers a significant growth of a  $\text{SiO}_2$ -amorphous layer spatially limited to the illuminated area. The layer gives rise to a catastrophic break-down of the  $\text{LiB}_3\text{O}_5$ -output surface upon long-term laser operation even at intensities far below the laser-induced damage threshold. The interaction of UV laser light,  $\text{LiB}_3\text{O}_5$  surface and foreign atoms in the ambient atmosphere is discussed in the frame of a two-step process for surface-damage formation.

© 2007 Optical Society of America

**OCIS codes:** (140.3330) Laser damage; (140.3610) Lasers, ultraviolet; (160.3380) Laser materials; (190.4400) Nonlinear optics, materials.

---

## References and links

1. Chen, Ye, Lin, Jiang, Zeng and Wu, "Computer-Assisted Search for Nonlinear Optical Crystals," *Adv. Mater.* **11**, 1071–1078, (1999).
2. Z.S. Lin, J. Lin, Z.Z. Wang, C.T. Chen, and M.H. Lee, "Mechanism for linear and nonlinear optical effects in  $\text{LiB}_3\text{O}_5$ ,  $\text{CsB}_3\text{O}_5$ , and  $\text{CsLiB}_6\text{O}_{10}$  crystals," *Phys. Rev. B* **62**, 1757–1764, (2000).
3. C. Chen, Y. Wu, A. Jiang, B. Wu, G. You, R. Li, S. Lin, "New nonlinear-optical crystal:  $\text{LiB}_3\text{O}_5$ ," *J. Opt. Soc. Am. B* **6**, 616–621, (1989).
4. Y. Furukawa, S.A. Markgraf, M. Sato, H. Yoshida, T. Sasaki, H. Fujita, T. Yamanaka and S. Nakai, "Investigation of the bulk laser damage of lithium triborate,  $\text{LiB}_3\text{O}_5$ , single crystals," *Appl. Phys. Lett.* **65**, 1480–1482, (1994).
5. H. König and R. Hoppe, "Über Borate der Alkalimetalle II Zur Kenntniss von  $\text{LiB}_3\text{O}_5$ ," *Z. anorg. allg. Chem.* **439**, 71–79, (1978).
6. V.V. Atuchin, L.D. Pobrovsky, V.G. Kesler, L.I. Isaenko, and L.I. Gubenko, "Structure and chemistry of  $\text{LiB}_3\text{O}_5$  (LBO) optical surfaces," *J. of Cer. Proc. Res.* **4**, 84–87, (2003).
7. W.E. Morgan and J.R. Van Wazer, "Binding Energy Shifts in the X-Ray Photoelectron Spectra of a Series of Related Group IV-a Compounds," *J. Phys. Chem.* **77**, 964–969, (1973).
8. R.W. Andreatta, C.C. Abele, J.F. Osmundsen, J.G. Eden, D. Lubben and J.E. Greene, "Low-temperature growth of polycrystalline Si and Ge films by ultraviolet laser photodissociation of silane and germane," *Appl. Phys. Lett.* **40**, 183–185, (1982).
9. C. Licoppe, Y.I. Nissim and J.M. Moison, "Surface chemistry and growth modes in the photochemical deposition of silica films," *Phys. Rev. B* **45**, 6275–6278, (1992).
10. K. Awazu and H. Onuki, "Photoinduced synthesis of amorphous  $\text{SiO}_2$  with tetramethoxysilane," *Appl. Phys. Lett.* **69**, 482–484, (1996).
11. H. Takao, M. Okoshi and N. Inoue, " $\text{SiO}_2$  films fabricated by  $\text{F}_2$  laser-induced chemical deposition using silicone rubber," *Appl. Phys. A* **79**, 1567–1570, (2004).

12. M. Suto and L.C. Lee, "Quantitative photoexcitation study of SiH<sub>4</sub> in vacuum ultraviolet," J. Chem. Phys. **84**, 1160–1164, (1986).
13. F. Houzay, J.M. Moison and C.A. Sèbenne, "Surface localization of the photochemical vapor deposition of SiO<sub>2</sub> on InP at low pressure and room temperature," Appl. Phys. Lett. **58**, 1071–1073, (1991).
14. C. Muguruma, N. Koga, Y. Hatanaka, I. El-Sayed, M. Mikami and M. Tanaka, "Theoretical Study of Ultraviolet Absorption Spectra of Tetra- and Pentacoordinate Silicon Compounds," J. Phys. Chem. A **104**, 4928–1935, (2000).
15. R. Waser, *Nanoelectronics and Information Technology*, (Wiley-VCH, Weinheim 2003).
16. W. Hong, M.M. Chirila, N.Y. Garces, L.E. Halliburton, D. Lupinski and P.Villeval, "Electron paramagnetic resonance and electron-nuclear double resonance study of trapped-hole centers in LiB<sub>3</sub>O<sub>5</sub> crystals," Phys. Rev. B **68**, 094111, (2003).
17. C.R.A. Catlow, S.A. French, A.A. Sokol and J.M. Thomas, "Computational approaches to determination of active site structures and reaction mechanisms in heterogeneous catalysts," Phil. Trans. R. Soc. A **363**, 913–936, (2005).
18. S. Stolbov and T.S. Rahman, "Alkali-Induced Enhancement of Surface Electronic Polarizability," Phys. Rev. Lett. **96**, 186801, (2006).

Borate crystals represent the most outstanding NLO materials for the generation of high-power ultraviolet laser light via frequency conversion since they offer distinctive nonlinear coefficients, sufficient transparency in the ultraviolet spectral range and a comparably high laser-induced damage threshold (LIDT) [1, 2, 3]. This is true in particular for lithium triborate (LiB<sub>3</sub>O<sub>5</sub>, LBO) with an absorption coefficient of  $\alpha \ll 0.1 \text{ cm}^{-1}$  over a broad spectral range of  $\lambda = 160 - 2600 \text{ nm}$  and values for LIDT up to  $25 \text{ GW/cm}^2$ . The threshold behavior of LBO was first determined in the work of Chen *et al.* [3] and Furukawa *et al.* [4] by exposure to single intense ns-laser pulses. Bulk and surface damages were separately induced for the wavelengths  $\lambda = 1064, 532$ , and  $355 \text{ nm}$ , which appear simultaneously in LBO when applied for sum-frequency generation. Despite of these values for the *direct* light-induced opto-mechanical breakdown of the crystals, i. e., damages appearing immediately after exposure, no investigations have been reported for the damage behavior of LBO during long-term sum-frequency generation with ns-laser pulses.

In this letter, we report on our investigations of the surface properties of LBO during long-term (up to 500h) sum-frequency generation (SFG) of  $\lambda = 355 \text{ nm}$  at intensities well below the direct LIDT in LBO. Damage formation on the optical output surface is visualized as a function of exposure using low-coherence (LCM) and atomic-force microscopy (AFM). Amorphous layer deposition is uncovered at low exposure, which is analyzed by electron spectroscopy for chemical analysis (ESCA). A two-step process of UV-promoted deposition and subsequent ablation of amorphous layers, containing SiO<sub>2</sub> in our case, is proposed and we discuss our findings by considering the mutual interaction of UV laser light, LiB<sub>3</sub>O<sub>5</sub> surface, and foreign atoms in the ambient atmosphere.

Our investigations were performed with plates of LBO single crystals purchased from the *Molecular Technology (MolTech) GmbH* having typical dimensions of  $5 \times 5 \times 1 \text{ mm}^3$ . The orthorhombic crystals (space symmetry group Pna2<sub>1</sub> [5]) were cut for type-II SFG of  $355 \text{ nm}$  with input wavelengths  $\lambda = 1064 \text{ nm}$  and  $532 \text{ nm}$ . The tilt angle was chosen to  $\phi = 43.6^\circ$  and both optical interfaces were polished to optical quality. Generation of  $355 \text{ nm}$  laser pulses was performed via SFG. Both fundamental and harmonic waves of a Q-switched frequency-doubled YVO<sub>4</sub>:Nd laser (Coherent Inc., model *Vector 532-1000-20*, average power  $P_{1064} = 1.6 \text{ W}$ ,  $P_{532} = 1.0 \text{ W}$ , repetition rate  $f_{\text{rep}} = 20 \text{ kHz}$ , pulse duration  $\tau_{1064} = 10 \text{ ns}$ ,  $\tau_{532} = 6 \text{ ns}$ ) were focused into the LBO crystal plate. We note that the intensities of the respective beams were chosen well below the reported values for the direct LIDT even in the focal point ( $I_{1064} < 0.3 \text{ GW/cm}^2$ ,  $I_{532} < 1 \text{ GW/cm}^2$ ). The generated third harmonic wave was separated from the transmitted fundamental and second harmonic waves using two quartz prisms. The LBO crystal itself was mounted onto a temperature-controlled Cu-holder in order to precisely adjust the crystal temperature to  $T = (65 \pm 1)^\circ\text{C}$ . With this setup an average UV power of

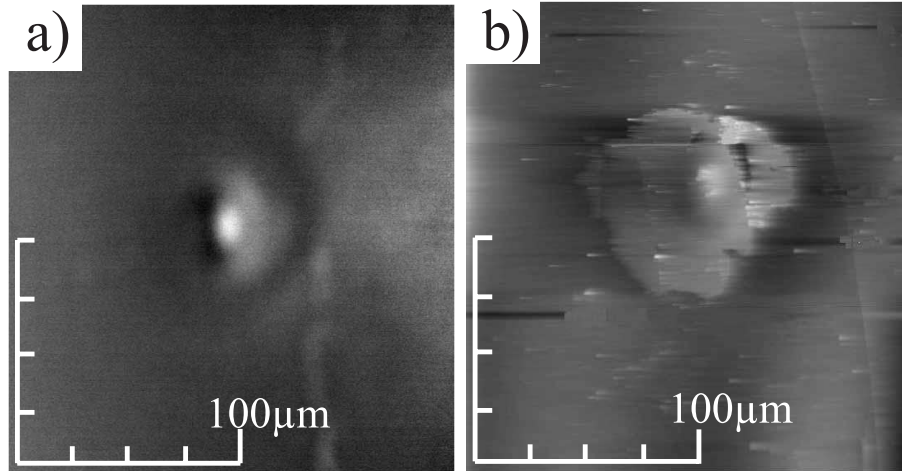


Fig. 1. Microscopic images of the LBO output surface after an SFG-exposure of 192 hours: a) determined by LCM, and b) determined by AFM.

$P_{355} \approx (15 \pm 1)$  mW was reached.

The LBO output surface was visualized by LCM (model *Mirau-WLI*, Breitmeier Messtechnik GmbH), with a lateral resolution of  $\leq 2 \mu\text{m}$  and of  $\leq 5 \text{ nm}$  in  $z$ -direction, respectively. In order to precisely position the microscope for investigations of the exposed area of the crystal output surface, the LCM was mounted within the experimental setup behind the sample. The absolute beam and spot position were determined from the microscopic image at lowest magnification with respect to the crystal boundaries. To avoid laser-damage of the LCM during SFG-exposure, the transmitting laser light was deflected-off using a mirror. Figure 1(a) exemplarily shows the LBO output surface after an SFG-exposure of 192 hours. A pronounced spot becomes visible which expands within an area of  $\approx 75 \mu\text{m}$  diameter. The spot position unambiguously corresponds with the surface area exposed to light during SFG. To verify the topographic data-set, the surface was additionally scanned by AFM (model *Q-Scope 250*, Quesant Instr. Corp.) with a comparable spatial resolution of  $\Delta x = \Delta y = 0.5 \mu\text{m}$ , as shown in Fig. 1(b). An equivalent image set was obtained.

LCM investigations were performed repeatedly in intervals of 24 hours and height profiles cutting the spot center were determined from the particular data sets (see Fig. 2). The surface profile taken at the beginning of exposure relates to a mean-surface roughness of  $\approx \pm 10 \text{ nm}$  of the LBO sample indicated by the dotted lines. As a function of SFG-exposure an elevation of the LBO surface within the exposed area becomes visible. A mono-exponential growth of the spot's height is found (see right insert) and the data points are fitted by  $A_o(1 - \exp(-t/\tau))$  yielding a saturation amplitude  $A_o = (286 \pm 10) \text{ nm}$  and a characteristic time constant of  $\tau = (54 \pm 20) \text{ h}$ . At the same time, the volume of the spot increases linearly with exposure, i.e. the spot area expands upon saturation of its height. The chemical composition of the grown spot was analyzed subsequently to SFG-exposure by ESCA (model *PHI 5600ci MultiTechnique XPS System*, Physical Electronics) using  $\text{Al K}\alpha$  radiation with a photonenergy of 1486.6 eV. The analysis was performed with MultiPak software (PHI) applying a Shirley type background. The striking results for a spatially limited area of  $\approx 400 \mu\text{m}$  diameter of an LBO surface after 100 hours of SFG-exposure are given in table 1. For reasons of comparison, one area covering the regime of surface elevation (*exposed*) as well as an unaffected (*unexposed*) area of the LBO

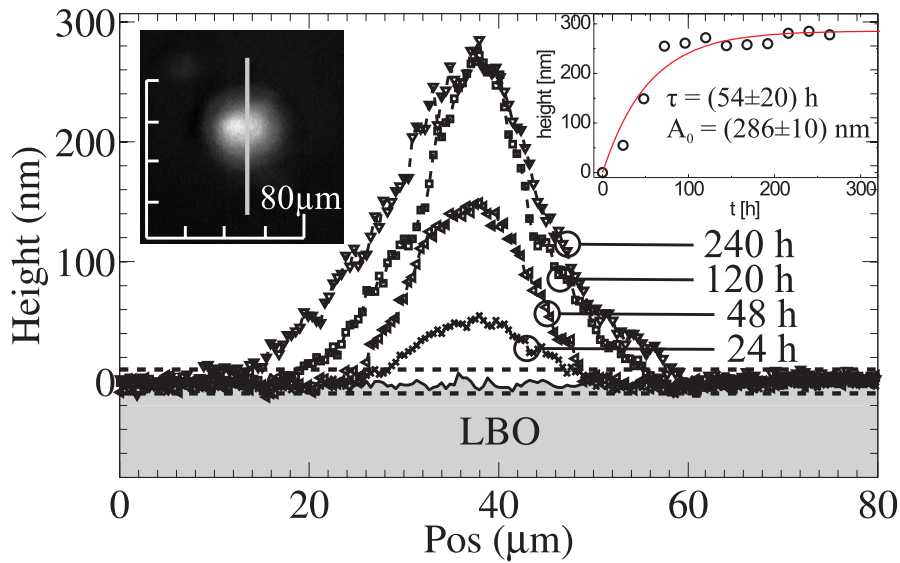


Fig. 2. Surface profiles of the LBO sample determined by LCM as a function of SFG-exposure exemplarily at the beginning ( $t = 0$ h) and after 24, 48, 120, and 240 hours. The data points were determined along the scan line shown in the inserted spot image. The horizontal dotted lines indicate the mean-surface roughness of the LBO crystal.

surface were investigated. The given values reflect the fraction of the particular element in

Table 1. Results of an ESC analysis for one area covering the regime of surface elevation (*exposed*) as well as an unaffected (*unexposed*) area of the LBO surface. The energetic positions of the determined peaks are referenced to the hydrocarbon-contaminant C (1s) line, assuming a value of 285.0 eV [7]. The values reflect the fraction of the particular element related to the total ESCA-signal (relative error  $\approx 10\%$ ). An increase of the peak at 103.9 eV by a factor of five is found in the exposed area.

peak center (eV)	56.7	193.1	532.4	348	103.9	1072.5
	Li	B	O	(Ca)	(Si)	(Na)
<i>unexposed</i>	9.9	31.0	57.6	0.5	0.5	0.5
<i>exposed</i>	9.2	27.7	58.8	0.3	2.3	1.0

relation to the totally determined ESCA-signal. Understandable pronounced concentrations of Li, B, and O proportional to the chemical composition of LBO were determined in both the exposed and unexposed areas. Impurities such as Na and Ca were determined with comparably low concentration. According to the results of Ref. [6], this contamination might be a result of the polishing and cleaning procedure of the surface. The respective peak intensities determined at different positions over the entire unexposed output surface varied by a factor of two. This magnitude of variation is found in the exposed area as well, and can therefore not be assigned to the action of light. In contrast, a significant increase of the peak at 103.9 eV by a factor of five in the exposed area is found which is very remarkable. The peak position can be assigned

to Si (2p) in a SiO<sub>2</sub>-configuration according to the results published in Ref. [7]. The spot in figure 1 therefore is identified as (amorphous) SiO<sub>2</sub>-layer grown under the simultaneous action of infrared, green and ultraviolet light.

Although the photo-assisted deposition of SiO<sub>2</sub> on LBO has not been reported in the frame of damage-formation mechanisms so far, the impact of UV light for deposition mechanisms of thin films of SiO<sub>2</sub> on various insulating and semiconducting surfaces has been investigated several years ago [8, 9]. In particular, ultraviolet-promoted chemical vapor deposition is now among the standard techniques. Effective growth processes are obtained using gaseous Si compounds (e. g., SiH<sub>4</sub> [9]), liquids (tetramethoxysilane [10]), or silicone rubber [11]. In either case, both reactant and substrate are illuminated with deep UV light ( $\lambda < 300\text{nm}$ ). Oxygen is supposed to be the second partner in the reaction. Evidences for photo-excitation of the reactants (Si compound and oxygen) as well as direct photo-excitation of the surface (depending on the substrate material), in particular with deep UV light, are further reported [9, 12, 13, 14]. These processes can be adopted to understand the discovered deposition of SiO<sub>2</sub> on LBO during SFG assuming the presence of foreign elements in the ambient atmosphere of our experimental setup, particularly of Si compounds. Their possible origin is manifold: It can be suggested that they appear via laser-ablation of Si compounds from the utilized optics, via outgassing from Si-containing wiring, or from Si-containing drying agents. Moreover, grinding or polishing of the crystal surface with SiC or Si-based material will result in the presence of Si compounds incorporated into the LBO surface. In general, the presence of foreign elements in the ambient atmosphere can only be excluded in ultra-high vacuum [15]. Reactants are excited by the SFG-generated ultraviolet light at 355 nm. In addition, light at  $\lambda = 178\text{nm}$  has to be considered which is generated in the LBO crystal due to frequency doubling of the third harmonic beam. Contrary, the contribution of infrared or green pump light can be neglected in these processes due to smaller photon energies. The LBO surface reactivity can be considered as well. Here, optically generated trapped hole polarons [16] might act as photocatalysts [17]. Moreover, it was reported only recently that adsorption of molecules on surfaces results in changes of the electronic properties of both molecules and surface. This additionally will facilitate excitation and will increase reactivity [18]. The particular concentration of foreign elements determined on the surfaces of our LBO samples hence is a direct fingerprint of the impurity content of the ambient atmosphere in our particular experimental setup. We suggest that SFG within a different atmosphere will result in changes of the characteristic time constant  $\tau$  and of the amplitude  $A_o$  related to the deposition process. However, it will not affect the deposition process in itself.

We now shortly discuss the role of the discovered deposition mechanism in the formation of optical damage. The grown SiO<sub>2</sub>-spot obviously will affect the beam-profile of the transmitted laser beam due to refraction processes. This beam distortion will become more and more pronounced with increasing spot dimensions. Indeed a deformation of the beam profile is observed in the far-field of the laser beam from the beginning of exposure in our experiment. The beam profile continuously deforms as a function of exposure which particularly reflects the volume growth of the spot. Remarkably, this process is limited: A sudden ( $< 5\text{ sec}$ ) and strong deterioration of the beam profile occurs, which is due to a catastrophic break-down of the LBO-surface. The surface topography according to such damage (see also e.g. Ref. [3]) is shown exemplarily in Fig. 3 for our LBO samples and optical setup. A crater-like surface structure exceeding by far the mean surface roughness of  $\pm 10\text{ nm}$  becomes visible. Such surface cracks predominantly occur at SFG-exposure  $\gg 500\text{ h}$ , or at high SFG-efficiencies, i. e., at high intensities of the ultraviolet laser beam. At low UV-intensities only fractions of the grown layer are ablated. To connect the SiO<sub>2</sub>-deposition process with the appearance of surface cracks, a two-step process of deposition and subsequent ablation of foreign material has to be assumed:

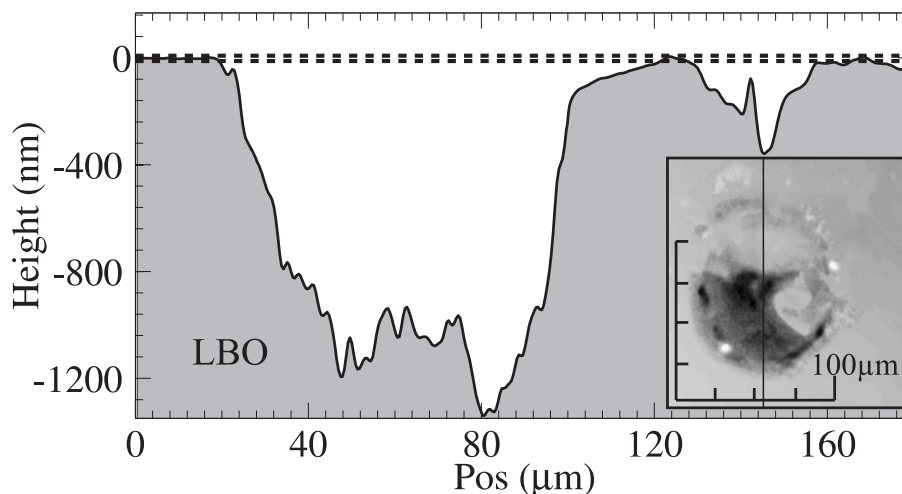


Fig. 3. Height profile of a cracked surface area related to the LCM-image shown in the insert. Such surface cracks predominantly occur at SFG-exposure  $\gg 500$  h, or at high SFG-efficiencies, i. e., at high intensities of the ultraviolet laser beam.

In the first step, foreign atoms are deposited on the LBO surface within the UV-exposed area yielding a layer formation, primarily containing  $\text{SiO}_2$  in substantial concentrations. Obviously, the UV absorbance of the deposited layer is considerably larger than that of LBO because of its impurity degree and amorphous growth. Together with the intense UV light, a considerable heating results and thermal ablation of the layer occurs. Remarkably, we observe that the ablation even strongly affects the subsurface and bulk of the LBO sample at high UV-intensities (Fig. 3). This points to a chemical bonding of the deposited layer with the LBO surface. We suggest that it is a result of a UV-induced excitation of the surface during the deposition according to the processes reported in Refs. [16, 18]. Hence, the role of the generated UV light is manifold and decisive in optical-damage formation on LBO surfaces.

Concluding our findings a two-step process of damage formation on LBO optical surfaces is discovered. LCM and AFM images of the LBO surface at various SFG-exposure together with ESCA investigations give strong evidence that the two steps are deposition and subsequent ablation of layers containing  $\text{SiO}_2$  during SFG. The layer formation most probably is promoted by UV-activated Si compounds and oxygen from the ambient atmosphere. The deposited layers are strongly bound to the LBO surface, thus indicating a direct excitation of the substrate by the UV light.

The above described damage process is neither specific for the investigated LBO material nor the surface polish since the deposition process appears in other LBO samples as well. Moreover, we are convinced that it is not limited to borate crystals, but is rather a general feature of oxidic NLO materials. Furthermore, this damage mechanism will be enhanced with increasing photon energy, for instance during fourth harmonic generation ( $\lambda = 266$  nm). Our findings are therefore of increasing importance for solid-state laser systems operating in the deep UV.

Financial support from the Deutsche Forschungsgemeinschaft within the Transferbereich 13 (project 13-04 / A5) is gratefully acknowledged.